

NATIONAL TRANSPORTATION SAFETY BOARD

Office of Research and Engineering
Materials Laboratory Division
Washington, D.C. 20594



3/21/2012

MATERIALS LABORATORY STUDY REPORT

Report No. 12-019

A. ACCIDENT INFORMATION

Place : Dubai, UAE
Date : 9/3/2010
Vehicle : Boeing 747-400F
NTSB No. : DCA10RA092

B. TOPICS ADDRESSED

- Fire load contribution of lithium and lithium-ion batteries
- Burning characteristics of aircraft cargo container fires

C. DETAILS OF THE STUDY

1. Fire load contribution of lithium and lithium-ion batteries

Lithium¹ and lithium-ion² batteries have been in the spotlight for the past few years due to their possible involvement in aircraft cargo fires. Recently there have been two in flight fire accidents in which the involvement of lithium and lithium-ion batteries has come into question. One of these accidents was UPS flight 1307, a McDonnell Douglas DC-8-71F which conducted an emergency landing on February 7, 2006, at Philadelphia International Airport. Although a successful emergency landing was made, the aircraft was a total loss by the time the fire was extinguished. Numerous fire-damaged batteries and battery-containing devices were found amongst the cargo, although no specific source was identified as the cause of the fire. The other accident with a possible lithium or lithium-ion battery involvement is UPS flight 6, a Boeing 747-400F which crash-landed on a military base in Dubai, United Arab Emirates (UAE) on September 4, 2010. This accident is currently under investigation by the General Civil Aviation Authority (GCAA) of the UAE. The preliminary report sites numerous shipments of batteries in the cargo manifest. One of the reasons batteries have been suspected in cargo fire incidents is due to the large number of instances where lithium and lithium-ion batteries in personal devices have been found to have led to a smoke, fire, or extreme heat event (FAA Office of Security and Hazardous Materials, 2011). In some situations, the causes of the batteries' failures were clear, such as shorting, mechanical damage and improper charging. In other situations, the cause was unknown.

¹ Lithium batteries are non-rechargeable (primary) cells containing lithium metal and a combustible electrolyte.

² Lithium-ion batteries are rechargeable (secondary) cells which have a combustible electrolyte but do not contain lithium metal.

To date, the hazard posed by lithium and lithium-ion batteries has not been fully understood and quantified by the fire protection community. A material or assembly of materials, as is the case in batteries, can have many characteristics that play a role in its ability to pose a fire hazard. Such characteristics can include, but are not limited to:

- High sensitivity to mechanical, thermal or electrical abuse
- Potential for thermal runaway
- The amount of energy released when burning
- Incendiary particles expelled during battery case rupture
- Pressure pulses associated with case rupture
- Toxic products of combustion
- Resistance to extinguishment

Some of these characteristics have been studied through previous experimentation, such as the behavior of both lithium and lithium-ion batteries when exposed to a small heat source (Webster, Flammability Assessment of Bulk-Packed, Nonrechargeable Lithium Primary Batteries in Transport Category Aircraft, June 2004). Additionally, there have been some experiments to evaluate the magnitude of the pressure pulse associated with energetic battery failures (Webster, Lithium-Ion and Lithium Metal Battery Update, October 27, 2010).

This portion of the study focused on quantifying the energy released per individual battery cell and then on quantifying the fire behavior of small quantities of batteries in different scenarios. The following table describes the test series in the battery portion of this study.

Test Series Name	Types of Batteries used	Test Scenario Description
Batteries#1	Lithium,lithium-ion, lithium-ion polymer	Individual battery cell fire tests using oxygen consumption calorimetry
Batteries#2	Lithium-ion 18650 type	Box of 100 batteries exposed to a propane burner simulating being a victim of an unrelated fire
Batteries#3	Lithium-ion 18650 type	Box of 100 batteries initiating a fire amongst ordinary combustibles

The focus of the tests in the Batteries#1 test series was to quantify the amount of energy released per single battery by conducting a series of small scale tests using lithium, lithium-ion and lithium-ion polymer batteries. Knowing this information can allow for the estimation of the amount of energy a certain number of batteries; for example, a package of batteries placed in cargo can contribute to a fire. Although it is expected that the total

energy is a summation of the energy potential of each battery cell in the shipment and therefore can be predicted, the actual rate at which this energy is released greatly depends on the configuration of the batteries and the thermal exposure they receive and cannot be determined solely based on the number of batteries present.

The energy contribution of lithium and lithium-ion batteries involved in a fire was evaluated by means of oxygen consumption calorimetry.³ The first series of tests was conducted using single battery cells (lithium, lithium-ion, and lithium-ion polymer⁴) at a time and they were conducted at the Fire Research Branch of the Federal Aviation Administration's Technical Center (FAATC) in Atlantic City, NJ. The second series of tests was conducted using single boxes of batteries (containing 100 lithium-ion batteries each) and were conducted at the Fire Research Laboratory of the Bureau of Alcohol Tobacco Firearms and Explosives (BATFE). The tests carried out at the FAATC were performed using an oxygen consumption calorimeter as described in the standard test method ATSM E-1354.⁵ The test involves subjecting a test specimen, in this case a battery cell, to a uniform external heat flux and then measuring the amount of oxygen consumed during the combustion of the test specimen. The mass of oxygen consumed is then related to the energy released during the combustion of the battery cell. The tests conducted at the BATFE were performed under exhaust hoods instrumented for oxygen consumption calorimetry.

The types of batteries used in these tests were of the lithium, lithium-ion, and lithium-ion polymer variety. These batteries are shown in table 1.

Table 1: Batteries tested

Manufacturer	Type	Model	Capacity
LG Chem Ltd Seoul, South Korea	Lithium-ion	18650	2600 mAh
Titanium Innovations inc Essex, CT	Lithium	CR2	unavailable
SureFire LLC Fountain Valley, CA	Lithium	SF123A	unavailable
Powerizer	Lithium-ion polymer	PL-553562-10C	1050 mAh
Powerizer	Lithium-ion polymer	PL-603495-10C	1900 mAh

³ Oxygen consumption calorimetry is a method of measuring a material's energy release rate during combustion by relating the amount of oxygen consumed to the energy released.

⁴ This type of battery has technologically evolved from lithium-ion batteries. The primary difference is that the lithium-salt electrolyte is not held in an organic solvent but in a solid polymer composite such as polyethylene oxide or polyacrylonitrile.

⁵ ASTM E-1354 Standard test method for heat and visible smoke release rates for materials and products using an oxygen consumption calorimeter.

1.a Battery tests at the FAATC (test series Battery#1)

The batteries tested at the FAATC using the ASTM E-1354 apparatus, also referred to as the “cone calorimeter” (due to the conically shaped heating element), were tested in duplicate with the heater set at $10 \frac{kW}{m^2}$, $30 \frac{kW}{m^2}$, $50 \frac{kW}{m^2}$ and $75 \frac{kW}{m^2}$. At $10 \frac{kW}{m^2}$ the battery behavior was erratic with instances of non-ignition of the expelled electrolyte or lack of violent battery venting⁶ altogether. In general, the behavior of all the types of batteries tested, with the exception of the lithium-ion polymer batteries, was to vent twice, and therefore an initial and final venting time was recorded during each test. The following tables (2 - 6) show the results from the tests.

Table 2: LG lithium-ion 18650 batteries

Battery Model	Heat Flux ⁷ ($\frac{kW}{m^2}$)	Initial Vent ⁸ (sec)	Final Vent ⁹ (sec)	Peak HRR ¹⁰ (kW)	Total HR ¹¹ (kJ)	Mass loss ¹² (g)	Heat of Combustion ¹³ ($\frac{kJ}{g}$)
18650	30	165	242	13.7	84	10.3	8.2
18650	30	166	242	9.8	76	12.6	6.0
18650	50	109	159	10.2	100.2	10.1	9.9
18650	50	96	137	16.2	92.8	9.6	9.7
18650	75	56	75	12.3	81.6	9.1	9.0
18650	75	50	71	16.2	92.5	9.1	10.2

⁶ Battery venting is the expulsion of electrolyte from the battery due to internal overpressure of the battery usually caused from the battery experiencing a thermal runaway.

⁷ Heat flux is the magnitude of the thermal exposure that the test specimen is subjected to.

⁸ Time after exposure to heat source that the initial vent occurred

⁹ Time after exposure to heat source that the final vent occurred

¹⁰ Peak HRR is the instantaneous peak heat release rate of the combusting sample. Also referred to as energy release rate.

¹¹ Total HR is the time integrated heat release rate of the test and represents the total amount of energy released during combustion. Also referred to as total energy release.

¹² Total mass of sample consumed during the test

¹³ The heat of combustion is the total heat release divided by the mass loss and represents the energy liberated per unit mass of combustible consumed.

Table 3: Titanium Innovations lithium CR2 batteries

Battery Model	Heat Flux ($\frac{kW}{m^2}$)	Initial Vent (sec)	Final Vent (sec)	Peak HRR (kW)	Total HR (kJ)	Mass loss (g)	Heat of Combustion ($\frac{kJ}{g}$)
CR2	30	115	148	2.8	27	3.3	8.2
CR2	30	118	161	3.1	32	3.2	10.0
CR2	50	77	85	3.9	20.3	3.4	6.0
CR2	50	90	118	3.7	33.1	3.5	9.5
CR2	75	54	65	6.5	33.5	2.3	14.6
CR2	75	54	70	4.2	31.4	3.7	8.5

Table 4: Sure Fire lithium SF123A batteries

Battery Model	Heat Flux ($\frac{kW}{m^2}$)	Initial Vent (sec)	Final Vent (sec)	Peak HRR (kW)	Total HR (kJ)	Mass loss (g)	Heat of Combustion ($\frac{kJ}{g}$)
SF123A	30	104	149	4.2	42	4.7	8.9
SF123A	30	113	149	3.6	55	8.4	6.5
SF123A	50	74	94	3.9	52.2	4.4	11.9
SF123A	50	69	89	4.7	73.5	4.4	16.7
SF123A	75	48	68	5.9	64	3.8	16.8
SF123A	75	52	67	3.5	44.6	4.3	10.4

Table 5: Powerizer lithium-ion polymer PL553562-10C batteries

Battery Model	Heat Flux ($\frac{kW}{m^2}$)	Initial Vent (sec)	Final Vent (sec)	Peak HRR (kW)	Total HR (kJ)	Mass loss (g)	Heat of Combustion ($\frac{kJ}{g}$)
PL-553562-10C	30	112	N/A	9.2	57	3.3	17.3
PL-553562-10C	30	130	N/A	8.9	47	2.9	16.2
PL-553562-10C	50	38	51	6	77	5.1	15.1
PL-553562-10C	50	48	63	5.7	75	5.6	13.4
PL-553562-10C	75	14	44	7.1	109	6.1	17.9
PL-553562-10C	75	22	31	5.8	97	7.2	13.5

Table 6: Powerizer lithium-ion polymer PL603495-10C batteries

Battery Model	Heat Flux ($\frac{kW}{m^2}$)	Initial Vent (sec)	Final Vent (sec)	Peak HRR (kW)	Total HR (kJ)	Mass loss (g)	Heat of Combustion ($\frac{kJ}{g}$)
PL-603495-10C	30	64	84	7.8	156	10.2	15.3
PL-603495-10C	30	68	88	7	145	9.8	14.8
PL-603495-10C	50	35	52	8	162	11.1	14.6
PL-603495-10C	50	35	58	5.8	147	11.1	13.2
PL-603495-10C	75	19	35	8.9	165	12.1	13.6
PL-603495-10C	75	22	39	7.4	170	12	14.2

Based on the data in tables 2 – 6, there does not appear to be a strong and consistent trend of increasing peak energy release rate with increasing heat flux applied to the sample. The mass loss, total heat release, and therefore heat of combustion remain fairly constant regardless of the heat flux applied to the sample. The average values of the previously tabulated results, across tests of all heat flux levels, are shown in the following table.

Table 7: Average values across all heat flux levels of measured test results

Battery Type	Average Peak HRR (kW)	Average Total HR (kJ)	Average Mass loss (g)	Average Heat of Combustion ($\frac{kJ}{g}$)
18650	13	88	10.1	8.7
CR2	4	29.5	3.2	9.2
SF123A	4.3	55	5.8	9.5
PL-553562-10C	7.1	77	5.8	13.3
PL-603495-10C	7.5	157.5	11	14.3

Example plots of the time resolved heat release rate of each type of battery tested follow. The remainder of the test results from the single cell battery tests can be found in appendix A.

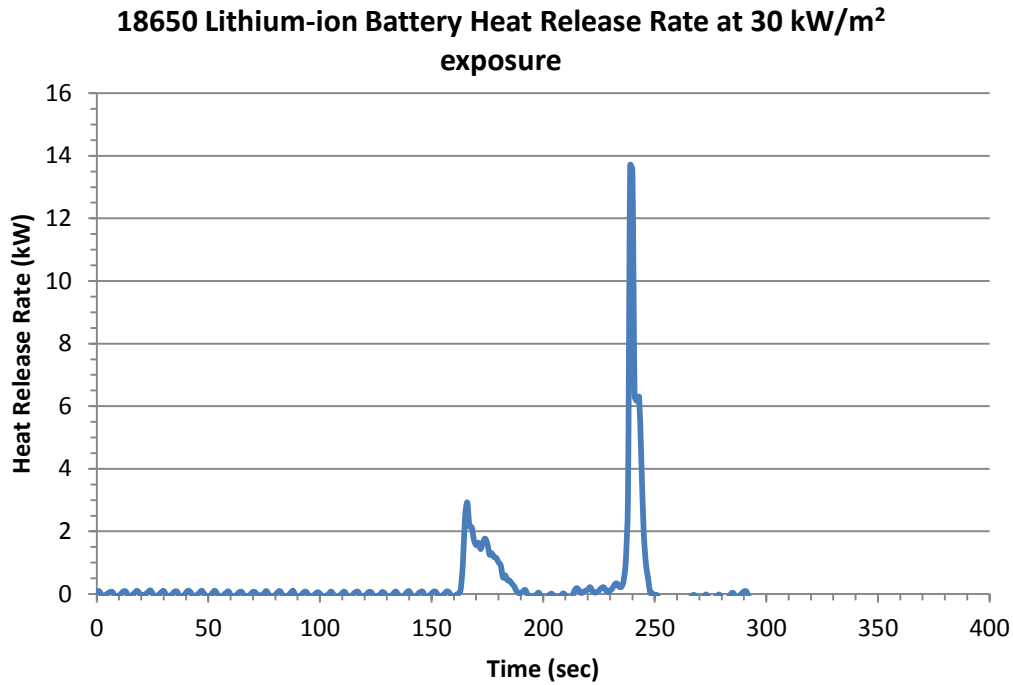


Figure 1: Heat release rate from a single 18650 battery exposed to a heat flux of 30 kW/m²

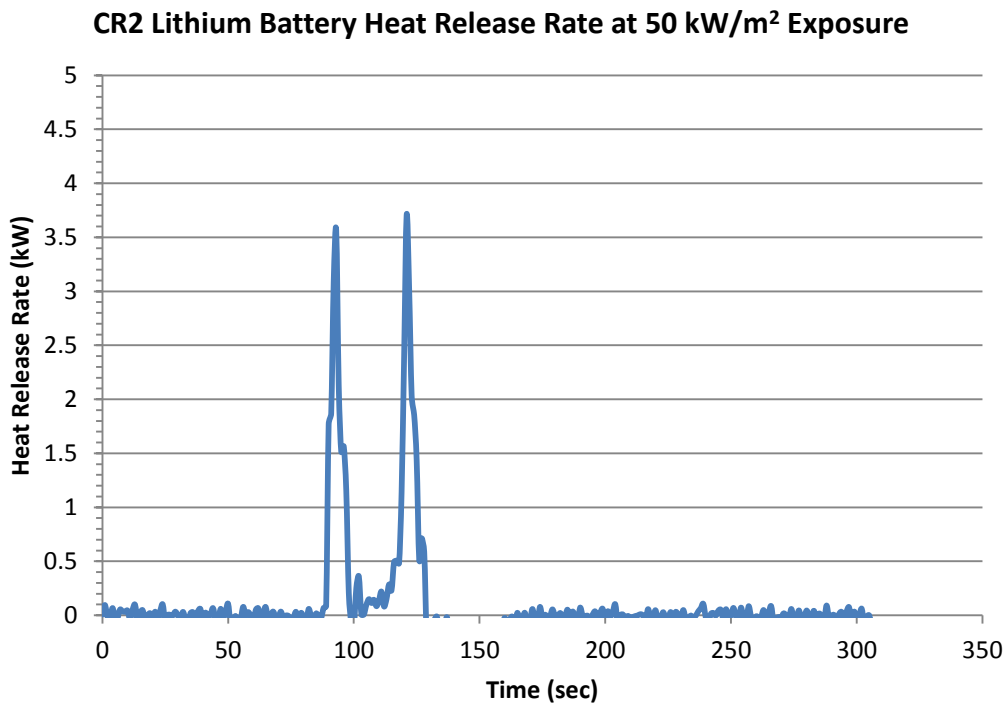


Figure 2: Heat release rate from a single CR2 battery exposed to a heat flux of 50 kW/m²

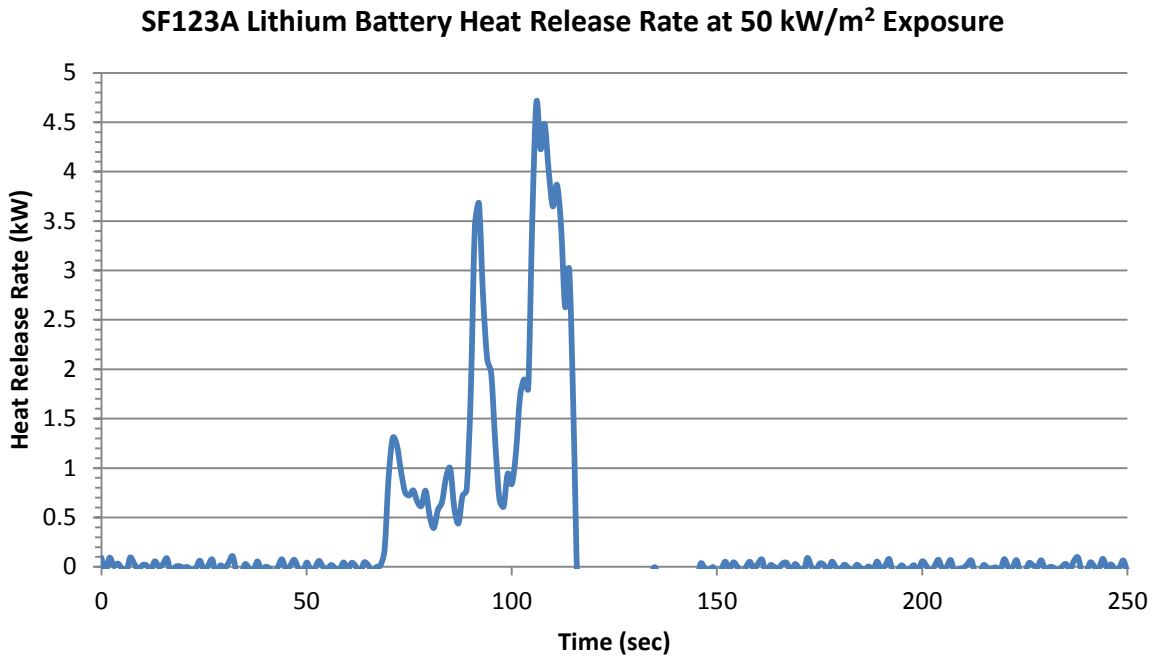


Figure 3: Heat release rate from a single SF123A battery exposed to a heat flux of 50 kW/m²

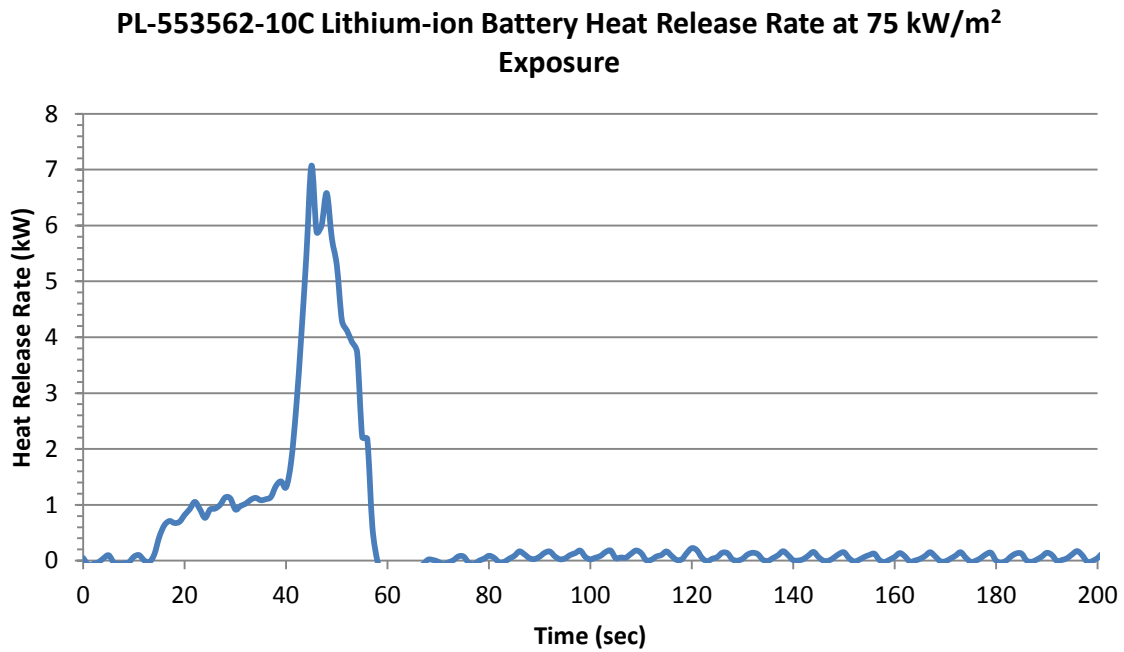


Figure 4: Heat release rate from a single PL-553562-10C battery exposed to a heat flux of 75 kW/m²

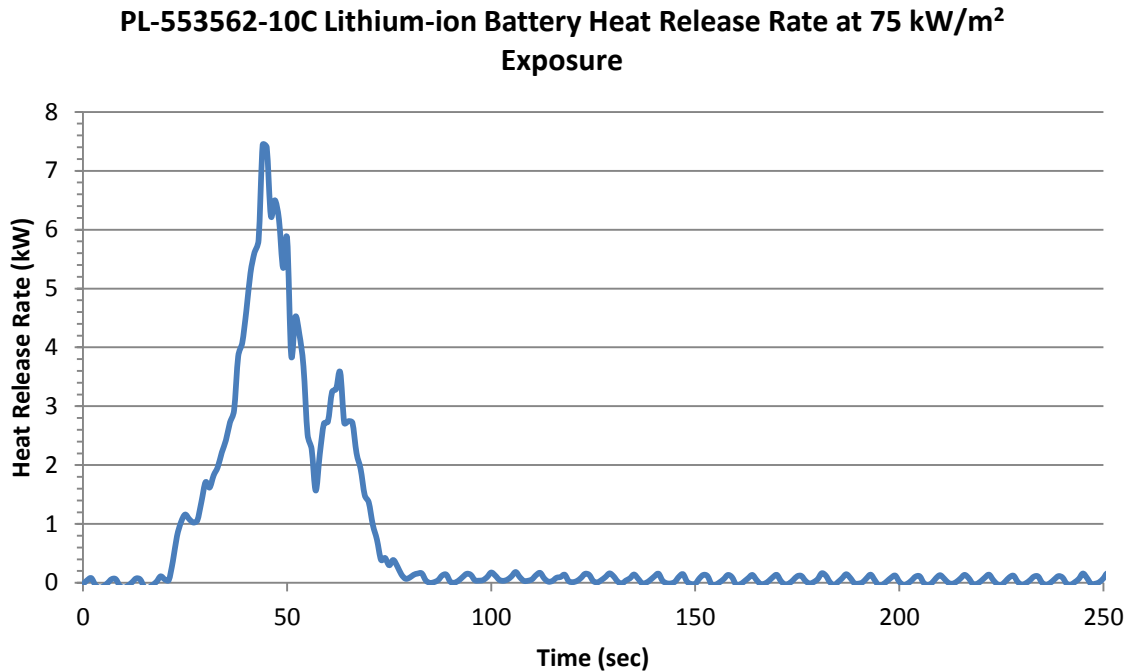


Figure 5: Heat release rate from a single PL-603495-10C battery exposed to a heat flux of 75 kW/m²

In the case of lithium-ion (and lithium-ion polymer) batteries, the combustible substance is limited to the electrolyte within each cell since there is no lithium metal present. The heat of combustion calculated from these experiments represents the heat of combustion of the electrolyte which was found to be $8.7 \frac{kJ}{g}$ for the 18650 type batteries and an average of $13.8 \frac{kJ}{g}$ for the two types of lithium-ion polymer batteries tested. In the case of the lithium (primary) batteries tested, the combustible substances are both the electrolyte and lithium metal. The combined heat of combustion of both substances was found to be on average, for both types of lithium batteries, $9.3 \frac{kJ}{g}$. These heats of combustion are lower than those of ordinary cellulosic materials such as newspaper $19.7 \frac{kJ}{g}$ ¹⁴ and significantly lower than those of typical combustible & flammable fluids which vary in the range of $35 \frac{kJ}{g}$ to $45 \frac{kJ}{g}$ ¹⁵. If the heat of combustion were to be calculated based on the overall mass of the battery rather than the mass loss, then the heats of combustion for the batteries tested are even lower as shown in the following table.

¹⁴ SFPE handbook 2nd edition, Appendix C, Table C-4.

¹⁵ SFPE handbook 2nd edition, Appendix C, Table C-4.

Table 8: Heat of combustion based on total mass

Battery Type	Average Total HR (kJ)	Average total mass (g)	Heat of Combustion based on total mass ($\frac{kJ}{g}$)
18650	88	43.5	2
CR2	29.5	10.5	2.8
SF123A	55	16.4	3.3
PL-553562-10C	77	23.3	3.3
PL-603495-10C	157.5	41.3	3.8

Although the sensitivity to thermal abuse was not the focus of this study, plotting the results of the time to the first vent versus the incident heat flux (figure 6) of each test and fitting the data to exponential curves produces a graph suggesting a critical heat flux (CHF)¹⁶ for lithium-ion battery failure of approximately $5 \frac{kW}{m^2}$ for the types of batteries tested in this study. This number is based on limited data and the tests were terminated after 15 minutes without battery failure. With more tests at heat flux levels around the established CHF and longer test durations, this number could be further refined.

¹⁶ Critical heat flux (CHF) is the limiting incident heat flux on a material below which ignition will not occur.

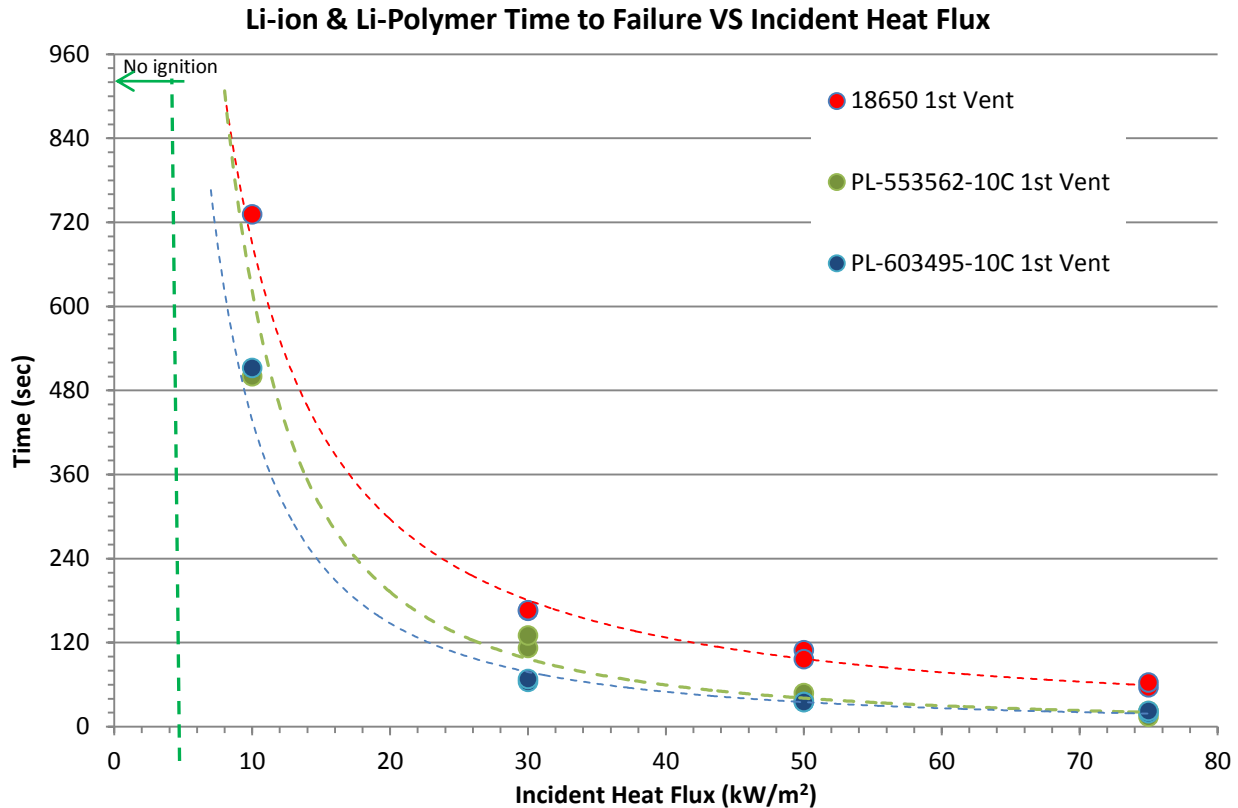


Figure 6: Battery failure time versus incident heat flux

1.b Battery testing at BATFE (test series Battery#2)

The tests in the series named Battery#2 and Battery#3 were conducted at the BATFE and burned under an exhaust hood instrumented for oxygen consumption calorimetry. Four tests were conducted, each using one box of 100 LG lithium-ion 18650 batteries. Series Battery#2 consisted of two tests that were carried out using a propane burner beneath the batteries to initiate the fire, and series Battery#3 consisted of two tests using a cartridge heater within the box of batteries to initiate the fire. The first case represents of a box of batteries exposed to an unrelated heat source and the second case represents a box of batteries self igniting.

In the case of exposing the box of batteries to a propane burner flame, the test setup is shown in figure 7. The box of batteries was placed on a stand constructed of angle iron which straddled the propane burner. The propane burner was controlled through a computer and a mass flow controller so that a steady output of 30 kW could be maintained throughout the test. On all four sides of the box of batteries, 22 inches away, were water-cooled Gardon type heat flux gauges. Adjacent to the box of batteries and extending vertically was a thermocouple “tree” to record temperatures in the fire plume above the batteries.

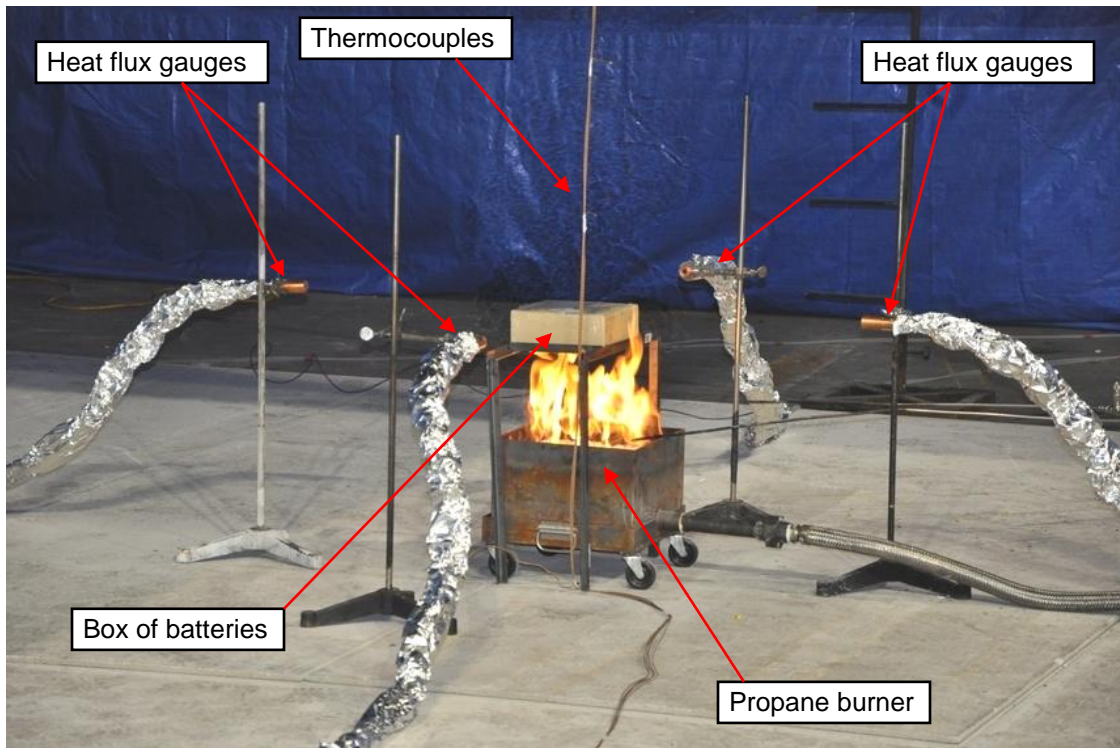


Figure 7: Test setup for batteries exposed to an unrelated fire

A graph showing the time resolved energy release rate of an example test is shown in figure 8. A red horizontal dotted line on the graph indicates the level of the energy output from the propane burner. At the beginning of the test, the measured energy output is briefly 30 kW and grows to 40 kW, where it remains for a few minutes before the batteries begin to get involved. This 10 kW excursion above the burner output prior to the batteries getting involved is likely the energy release due to the burning of cardboard box containing the batteries. The timeframe where the batteries are venting and burning lies between 340 seconds and 660 seconds, as indicated by the dotted vertical lines on the graph. After the batteries are all consumed, the energy release rate goes back to approximately 30 kW. During its peak contribution to the fire, the box of batteries increased the energy release rate by 90 kW. The energy associated with the combustion of the batteries is the area under the energy release rate graph in the interval between 340 seconds and 660 seconds, minus the energy from the propane burner during the same time interval. That results in 11237 kJ for the box of 100 18650 type lithium-ion batteries or 112.4 kJ per battery. From the previous tests at the FAATC, the measured energy for the same type of battery was measured slightly lower at 88 kJ per battery. The discrepancy is likely due to differences in instrument sensitivity between the small scale cone calorimeter and large scale 1 MW hood calorimeter used for the tests at BATFE as well as possible small variations of the propane burner output.

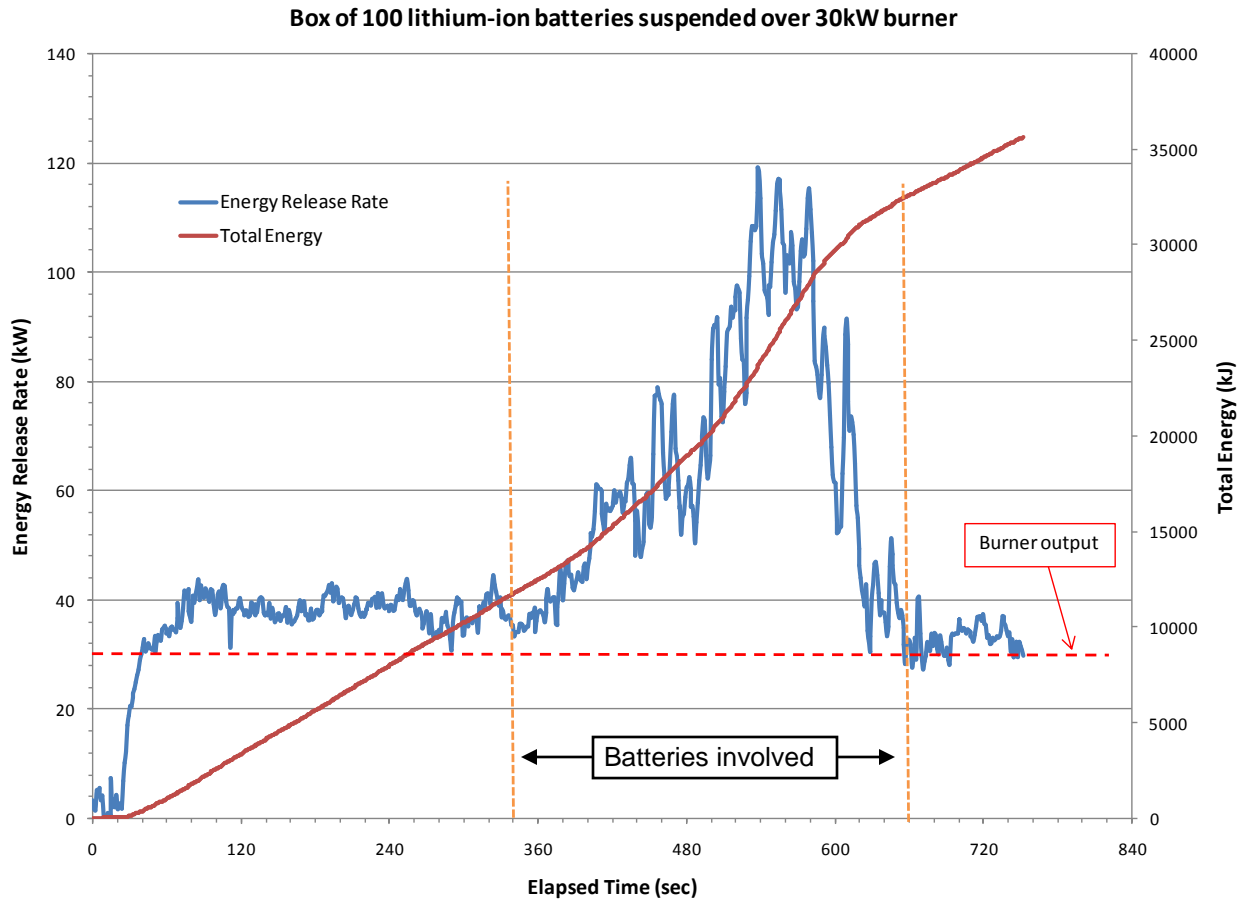


Figure 8: Graph of energy release rate and total energy

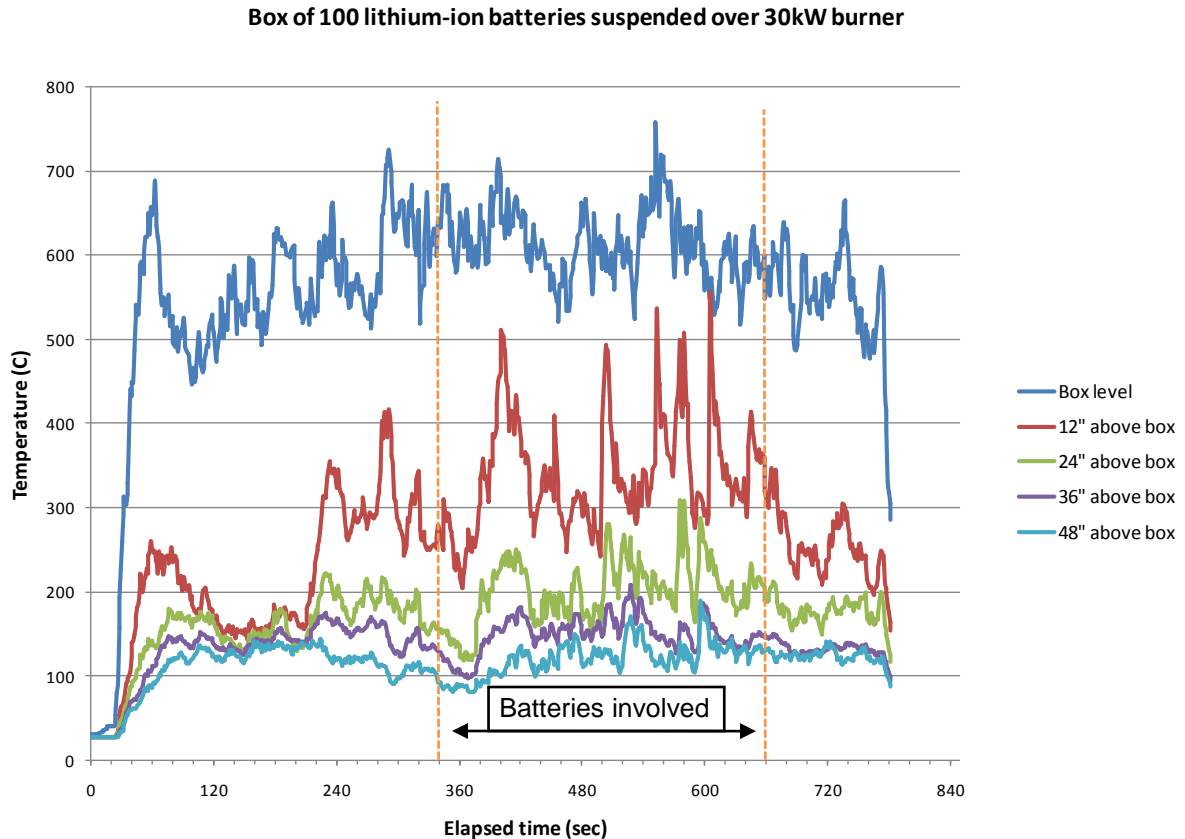


Figure 9: Graph of fire plume temperatures

The temperatures recorded during the test are shown in figure 9. The thermocouples were 24-gauge exposed bead type K thermocouples positioned in 12" increments vertically above the box of batteries with the first thermocouple being at the level of the box. The time interval during which the batteries were involved was between 340 seconds and 660 seconds as indicated by the vertical dotted lines on the graph. The overall plume temperatures were only affected at the 12-inch and 24-inch levels above the box of batteries. At those levels, the thermocouples appear to have been affected by the bursts of directional flames coming from the battery cells (figure 10) as evidenced by the temperature spikes recorded. The heat flux measurements are shown in figure 11. The peak heat flux recorded during the interval of battery involvement was just over $5 \frac{kW}{m^2}$ which represents an increase of about $3 \frac{kW}{m^2}$ above the heat flux due to the propane burner and burning cardboard alone.

Due to the violent nature of the battery case venting and combustion of the electrolyte, some of the batteries (or battery components) were liberated from the charred packaging and propelled several feet, landing onto the floor. Some of these projectiles continued to burn upon landing.



Figure 10: Box of lithium-ion batteries burning over propane burner exhibiting battery venting and electrolyte combustion

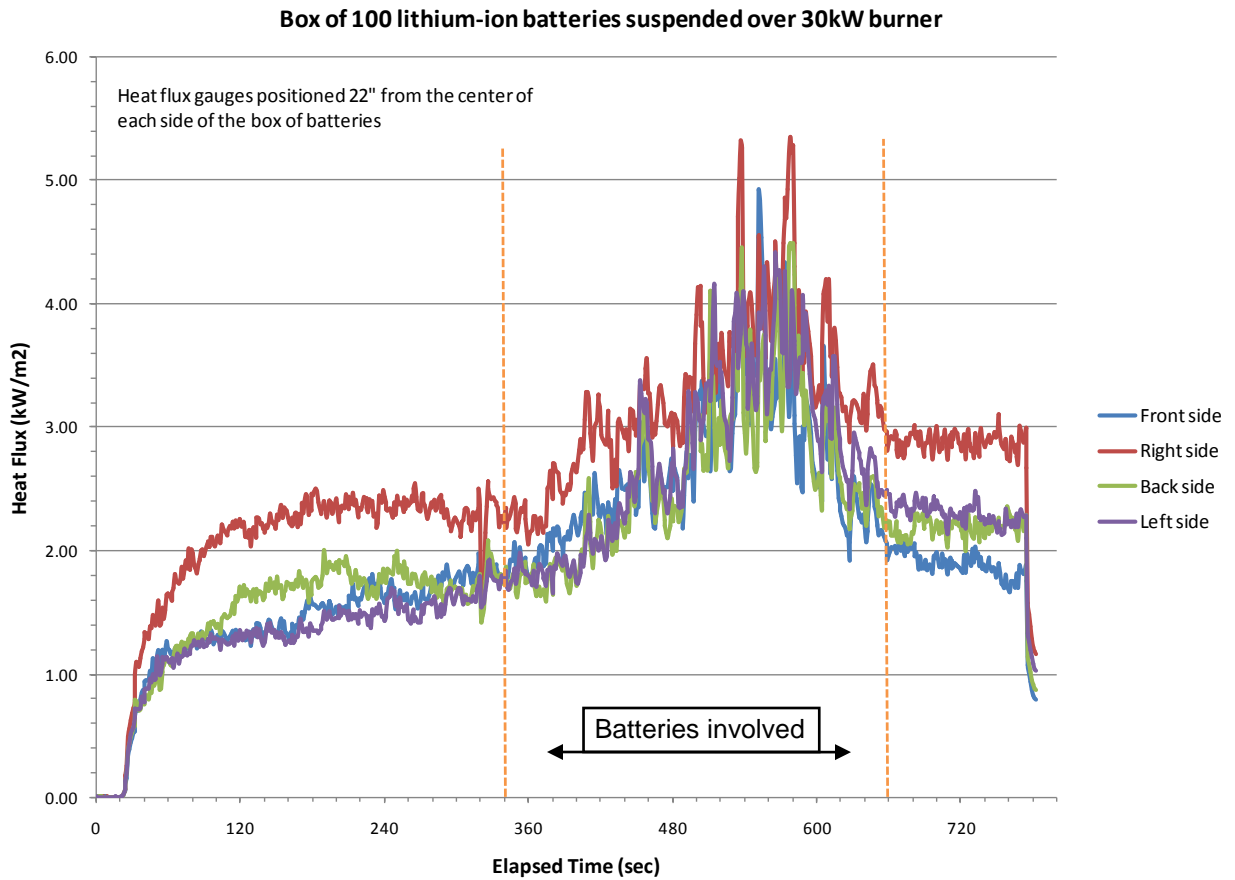


Figure 11: Graph of radiant heat flux measurements

To simulate the case of batteries being the cause of the fire and self-igniting, a 250-watt cartridge heater was used to simulate a battery going into thermal runaway. One cell in the corner of the box of 100 batteries was replaced by the cartridge heater (figure 12). In addition to the batteries, the fire load for each of the two tests included 18 cardboard boxes each containing 2.5 lb of shredded paper inside, arranged in a 3 x 3 array two levels high (figure 13). Each cardboard box was an 18" cube. The box of batteries was placed inside the cardboard box (and covered with 2.5lb of shredded paper) at the center of the top level of boxes in the array. The additional fire load was used to observe the battery thermal runaway spread to the rest of the combustibles and to determine if the presence of batteries in the fire load had any measurable effect. For reference, two control tests were conducted using 18 boxes and no batteries. Those fires were initiated by an electric match inside the cardboard box at the center of the top level of boxes in the array, just as in the tests that included the box of batteries.



Figure 12: Box of batteries with cartridge heater in place (circled in red)

In this test series (Battery#3), just as in the test with the box of batteries over the propane burner (Battery#2), radiant heat flux measurements and plume temperatures were recorded along with the oxygen consumption calorimetry. The test was run in duplicate. During the first iteration (test I), it appeared that the batteries vented without ignition of the expelled electrolyte until the very end, where it is unclear if the batteries or cartridge heater finally ignited the rest of the fire load. During the second iteration (test II), the vented electrolyte ignited early on in the test and actually caused a small explosion within the cardboard box in which the box of batteries was placed. The fire rapidly spread to the rest of the fire load and consumed it, leaving the batteries still venting and burning after all the

boxes were consumed. The difference between the two tests was that for the first one, the box of batteries was placed in between the center boxes of the lower and upper layers of boxes, and in the second test, the box of batteries was placed inside the center box of the upper layer.



Figure 13: Test setup for tests involving 18 cardboard boxes and one box of batteries

The graph of the energy release rates of both of the two tests involving cardboard boxes and batteries is shown in figure 14. On average, the tests involving the cardboard boxes and batteries had a peak energy release rate of 1.7 MW and a total energy of 298 MJ. The tests to which these results are to be compared to involved only cardboard boxes and no batteries. The results of these tests are shown in figure 15. On average, the tests involving just the cardboard boxes had a peak energy release rate of 1.6 MW and a total energy of 288 MJ. The tests involving the batteries did not exhibit any perceptible differences in the overall characteristics of the fires. Peak energy release rates were very similar and well within the variable nature of fire tests. The overall burning time of all the tests was also similar and was approximately 400 seconds. The average total energy of the tests which included the box of batteries was 10 MJ greater than the average of those tests that did not include the box of batteries. That difference is very close to the energy contribution of the box of batteries calculated from the propane burner tests. Temperatures measured in the fire plume of all these tests were also consistent regardless of the presence of batteries and peaked at $1000\text{ }^{\circ}\text{C} \pm 100\text{ }^{\circ}\text{C}$. The measured radiant heat flux also did not exhibit any significantly different results for the tests that included the batteries. The test reports from the BATFE containing all the test results for the battery tests with the propane burner and the battery tests with the array of cardboard boxes can be found in appendixes B and C respectively.

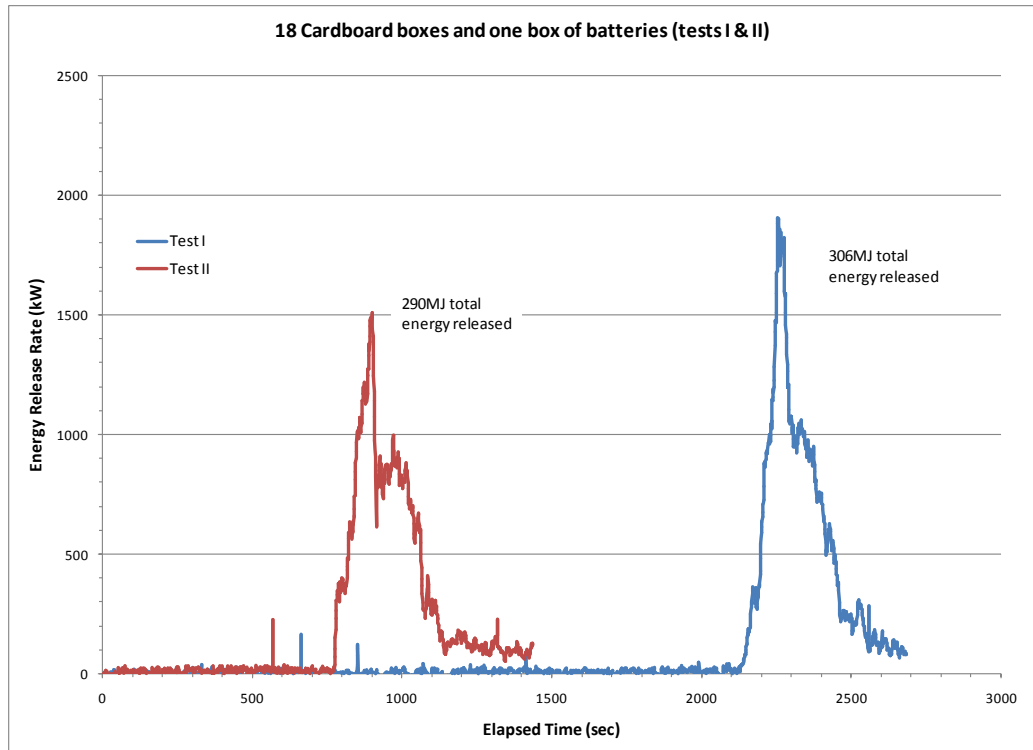


Figure 14: Energy release rate from tests involving cardboard boxes and batteries

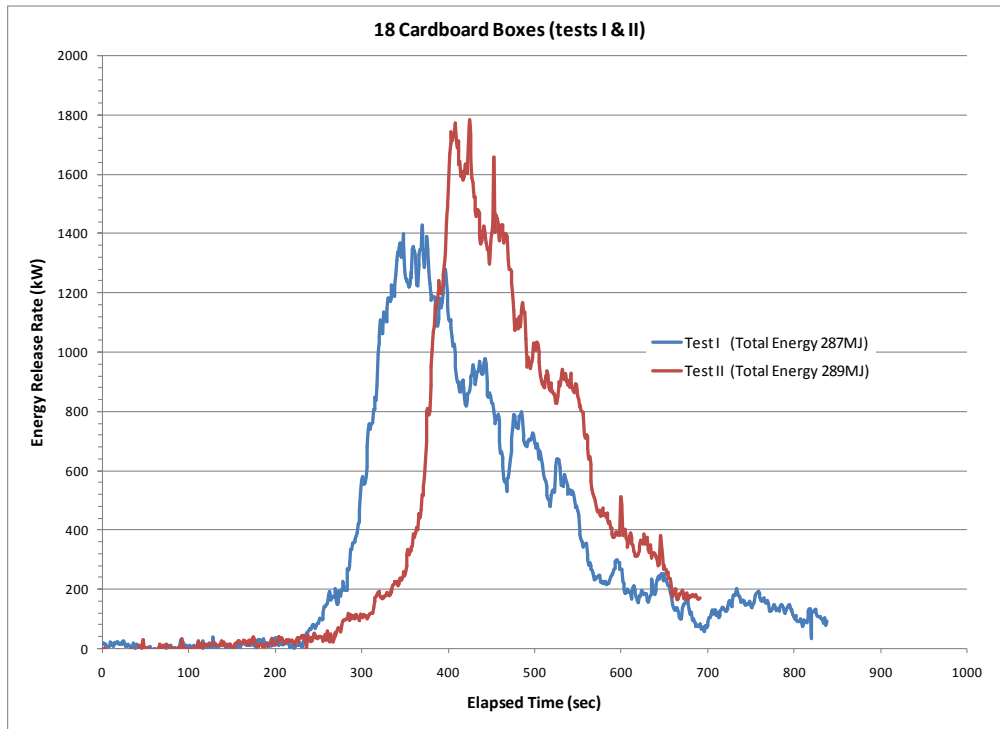


Figure 15: Energy release rate from tests involving cardboard boxes

2. Burning characteristics of aircraft cargo container fires

In the most recent freighter aircraft cargo fires, along with the speculation regarding the involvement of lithium and lithium-ion batteries, there have been questions among the aviation community relating to the overall characteristics of fires originating within cargo containers. These cargo fire accidents include the 2006 UPS flight 1307 in Philadelphia, PA, the 2010 UPS flight 006 in Dubai, UAE, and the 2011 Asiana flight 991 in South Korea. From the investigation of these recent accidents, there is evidence to suggest that there has been a short time frame from when a cargo fire is detected to when damage begins to occur to the aircraft's systems. This has been another reason why there is often speculation regarding the contribution of batteries to the severity of a cargo fire since there is a sense that aircraft are designed to withstand and contain an ordinary cargo fire.

In an effort to shed some light on the cargo fire problem and better understand why we are seeing catastrophic cargo fires, experiments were done to measure various characteristics of cargo container fires such as detectability, growth rate, and energy output. Once the characteristics of a cargo fire are known, then the appropriateness of the current fire protection strategies can be evaluated. Regulations in Title 14, *Code of Federal Regulations* (14 CFR) for fire protection of cargo impose certain burn-through requirements for liner materials (14 CFR 25.855). These burn through requirements only apply to the class C¹⁷ compartments and not to the large main deck class E¹⁸ compartments. Additionally, there are requirements for the certification of cargo compartments with aircraft-based smoke detection systems (14 CFR 25.858). Conversely, there are few requirements regarding fire protection for the design and materials used on cargo containers and how they impact the fire protection systems built into the aircraft, namely the smoke detection system.

It has been observed through visual examination of exemplars that the various types of cargo containers all have different paths from which smoke generated internally can exit the container and enter the space of the cargo compartment. None of these paths are designed intentionally for this purpose and they are simply artifacts of other design objectives. A visual examination of a large number of cargo containers at an air cargo sorting facility established that two types of cargo containers that may best exhibit the greatest possible range in cargo container fire performance are the rigid A2N¹⁹ type container and the collapsible DMZ²⁰ type container. Rigid containers are mostly built using aluminum and polycarbonate panels and usually have some type of fabric door. The door area generally offers the lowest resistance to smoke egress from the container (figure 17). The A2N type container looks like it would not greatly impede the movement of smoke from its interior to the open space of the cargo compartment. The collapsible type of container is

¹⁷ Class C cargo compartments have built-in fire suppression systems. These types of compartments are usually found on the aircraft's lower lobe.

¹⁸ Class E cargo compartments do not have fire suppression systems and are typically large main deck cargo compartments.

¹⁹ A2N is a cargo container size and configuration designation used within the United Parcel Service. The overall dimensions of an A2N container are 125" wide, 88" long and 81" tall.

²⁰ DMZ is a cargo container size and configuration designation used within the United Parcel Service. The overall dimensions of a DMZ container are 118" wide, 88" long and 95" tall.

erected for use when needed, similar to a cardboard box. In use, the collapsible container is covered with an impermeable material to act as a rain and dust shield. These types of containers, when covered, do not have well-established paths for smoke to pass through to the outside.

This portion of the study consisted of two test series, each with a different type of container (A2N and DMZ) to evaluate any delays in smoke egress from the containers from the time of the fire's initiation. Additionally, this portion of the study measured the time between when sufficient smoke egress from the container to activate an alarm and the time for the container fire to reach peak fire output.

The fire load chosen for these tests consisted of cardboard boxes containing 2.5lb of shredded paper inside. This is a fire load that has been used in past FAA fire tests and has been shown to be very repeatable. For example, the tests in the previous section of this study used arrays of 18 such cardboard boxes resulting in very good agreement between tests. Additionally, for future reference, since fire loads comprised of 18" cube cardboard boxes with 2.5lb of shredded paper inside are unofficially regarded as FAA "standard fire loads," experiments were performed on single boxes to quantify their total energy and energy release rate. These tests (appendix D) also exhibited good repeatability. Cargo containers can be packed with a wide variety of cargo shipments and the effect of that variability was beyond the focus of this study.

For all the tests conducted using cargo containers, a fire load consisting of 77 18" cube cardboard boxes with 2.5lb of shredded paper inside was used. The fire was initiated using a cartridge heater and a small fire log placed inside one of the cardboard boxes at floor level inside the cargo container. Measurements of energy release rate and total energy were made using an exhaust hood instrumented for oxygen consumption calorimetry. Heat flux measurements were taken at a distance of 60 inches from all four sides of the cargo container at a height of 66 inches from the ground. Temperature measurements above the container were made at distances of 12 inches, 24 inches, and 36 inches using type K thermocouples. In order to determine the time at which the smoke exiting the cargo containers would be sufficient to trigger an alarm from an aircraft's smoke detection system, the testing relied on two observers experienced in aircraft smoke detection system certification testing to make a determination of smoke concentration sufficient to trigger cargo bay smoke alarms.

2.a Rigid A2N container tests

Two tests were performed using the A2N type of rigid cargo container (figure 16). This container type is constructed from aluminum and polycarbonate and has a fabric roll-up door. The A2N container was chosen because it was likely to exhibit the shortest delay in becoming a detectable fire and because its materials of construction provide the least contribution to the fire load.

The results from both tests were in good agreement with each other. The peak energy release rates were 3.6 MW and 3.7 MW and the total energy released was 1530 MJ

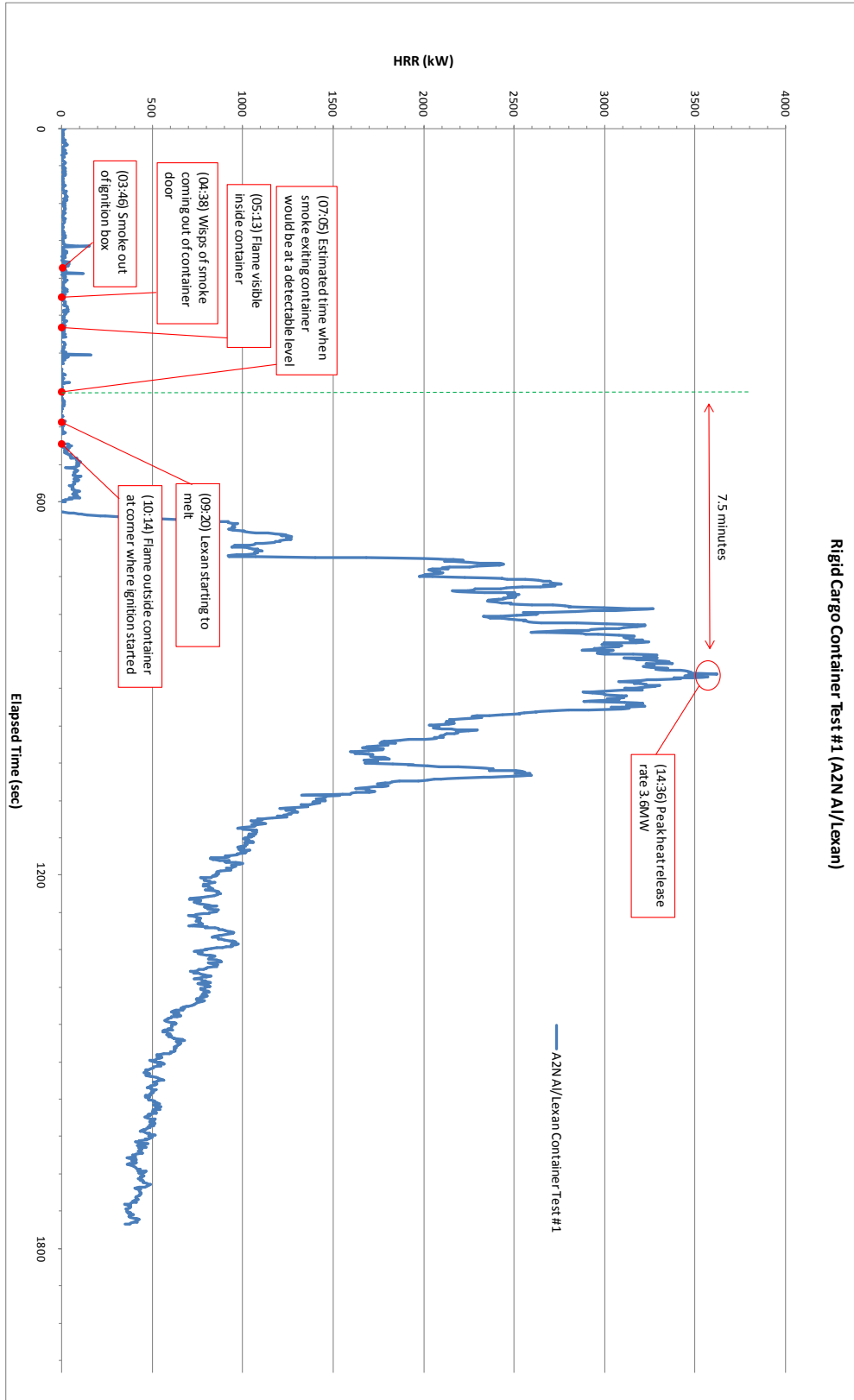
and 1690 MJ for tests 1 and 2, respectively. With regard to the smoke generation and its ability to exit the container, the observations made are noted on the graphs depicting the energy release rate of each test (figures 18 and 19). The first signs of smoke were observed to be exiting from the top portion of the roll-up door as expected. Two noteworthy time intervals are of particular importance. The first is the time between a fire being established inside the container and smoke beginning to exit the container in sufficient quantity to trigger an alarm, 199 seconds and 150 seconds for tests 1 and 2, respectively. The second is the time interval between the fire becoming detectable and the time to reach peak energy release rate, 450 seconds and 630 seconds for tests 1 and 2, respectively.



Figure 16: A2N type container with fuel load inside



Figure 17: Smoke exiting above roll-up door on A2N type container



Figure

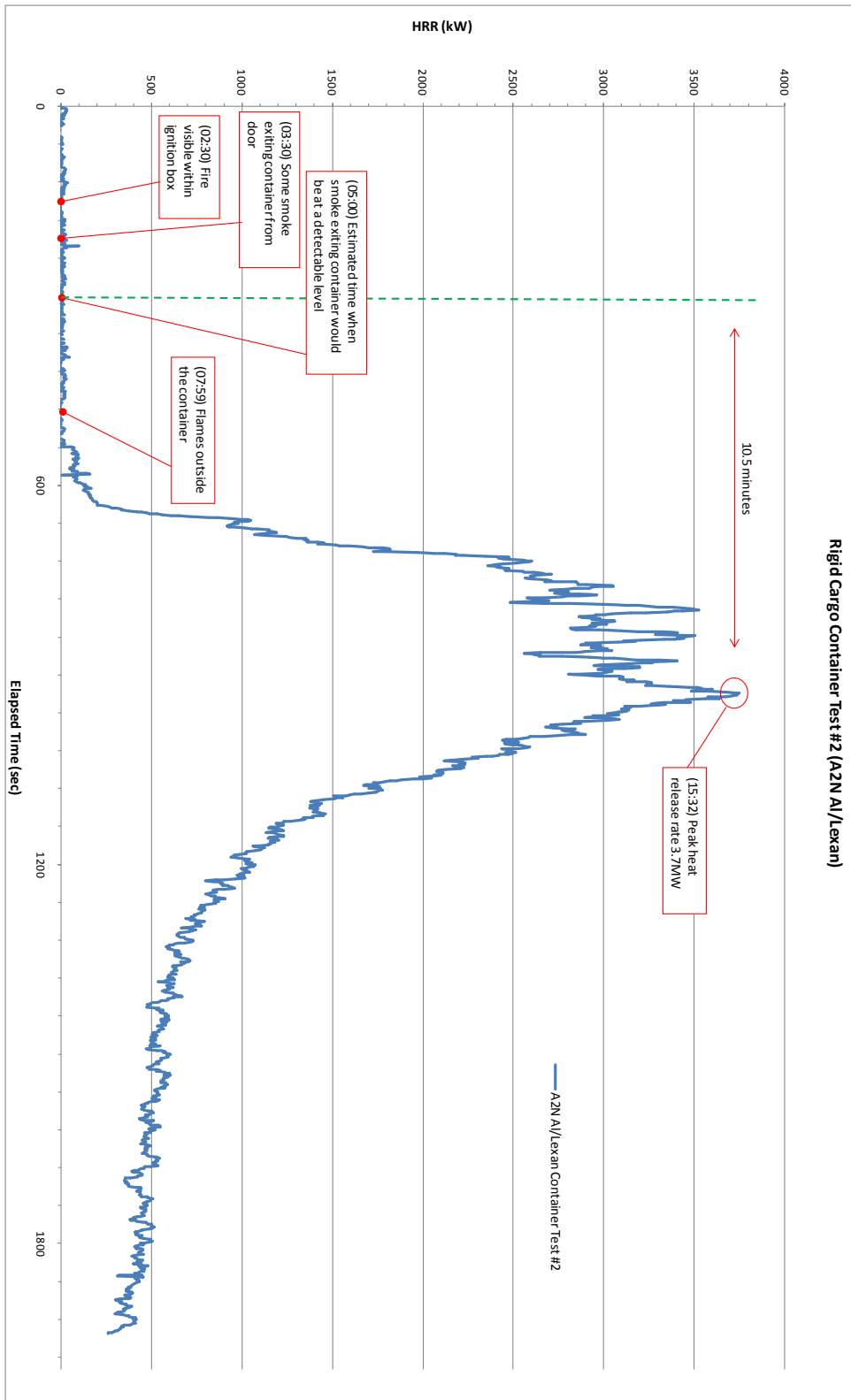


Figure 19: Energy release rate and observations from A2N container test 2

2.b Collapsible DMZ container tests

Two tests were performed using the DMZ type of collapsible cargo container (figure 20). This container type is constructed from corrugated polypropylene and while in use is covered with a lightweight impermeable cover. This container type was chosen because it was likely to exhibit the greatest delay in becoming a detectable fire and because the material of construction provide the most contribution to the fire load.

The results from both DMZ container tests were in good agreement with each other; however, in the first test, it took a longer time for the fire to begin to grow within the ignition box. The peak energy release rates were 8.5 MW and 7.2 MW and the total energy released was 1800 MJ and 3000 MJ for tests 1 and 2, respectively. Test 1 had a relatively smaller total energy release because the test was stopped early after the fire went into decline. For the second test, the fire was allowed to burn longer and thus the measured total energy was greater. With regard to the smoke generation and its ability to exit the container, the observations made are noted on the graphs depicting the energy release rate of each test (figures 21 and 22). An infrared camera was used inside the container to monitor the ignition and fire growth. The first signs of smoke were observed to exit the container and the plastic cover at floor level. The smoke exiting at floor level was no longer buoyant and remained at floor level. Two noteworthy time intervals are of particular importance. The first interval is the time between a fire being established inside the container and smoke beginning to exit the container in sufficient quantity to trigger an alarm, 18 min 30 sec and 5 min 10 sec for tests 1 and 2, respectively. The second interval is the time between the fire becoming detectable and the time to reach peak energy release rate, 132 seconds and 114 seconds for tests 1 and 2, respectively.



Figure 20: DMZ type container with plastic rain cover and cargo net

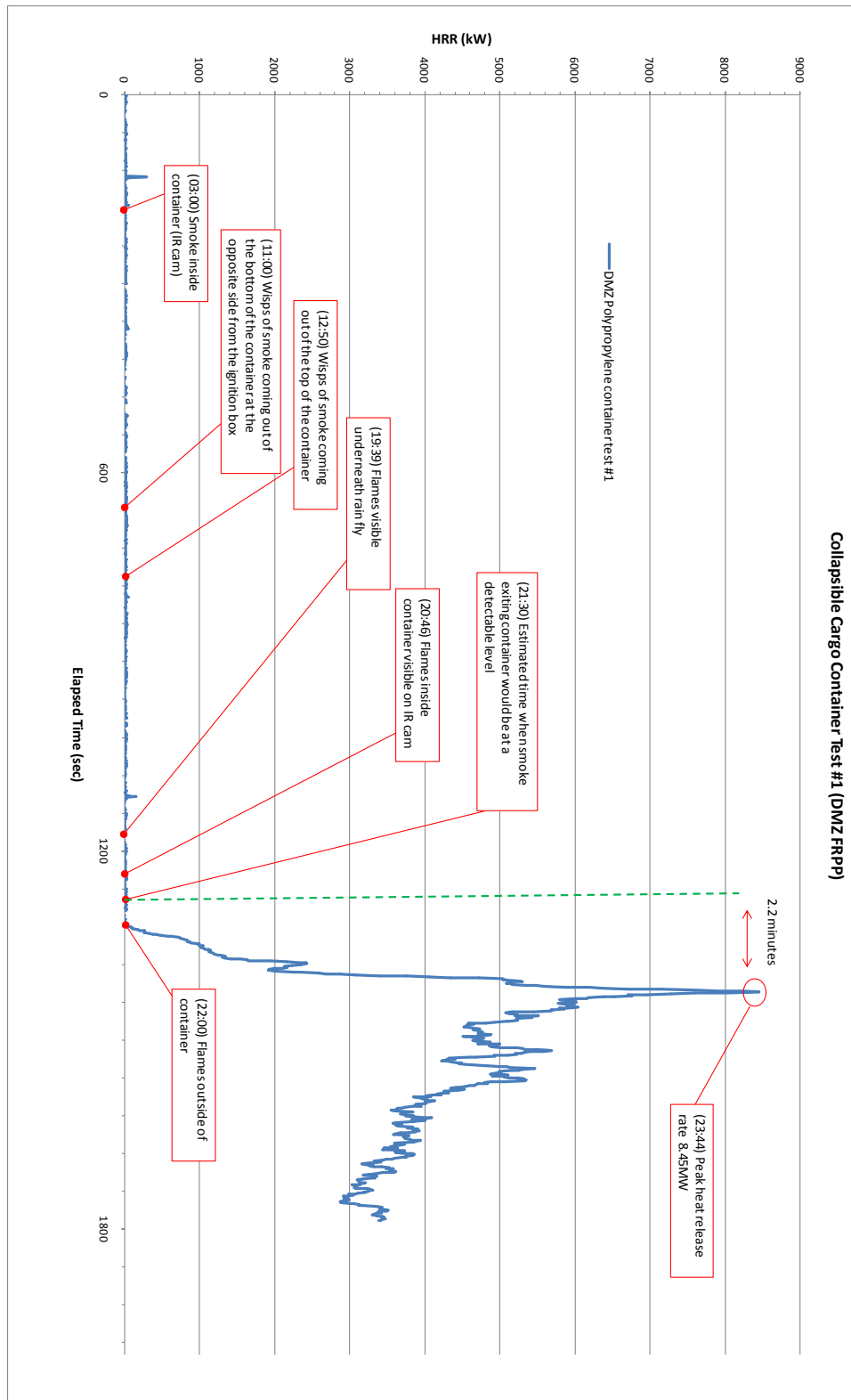


Figure 21: Energy release rate and observations from DMZ container test 1

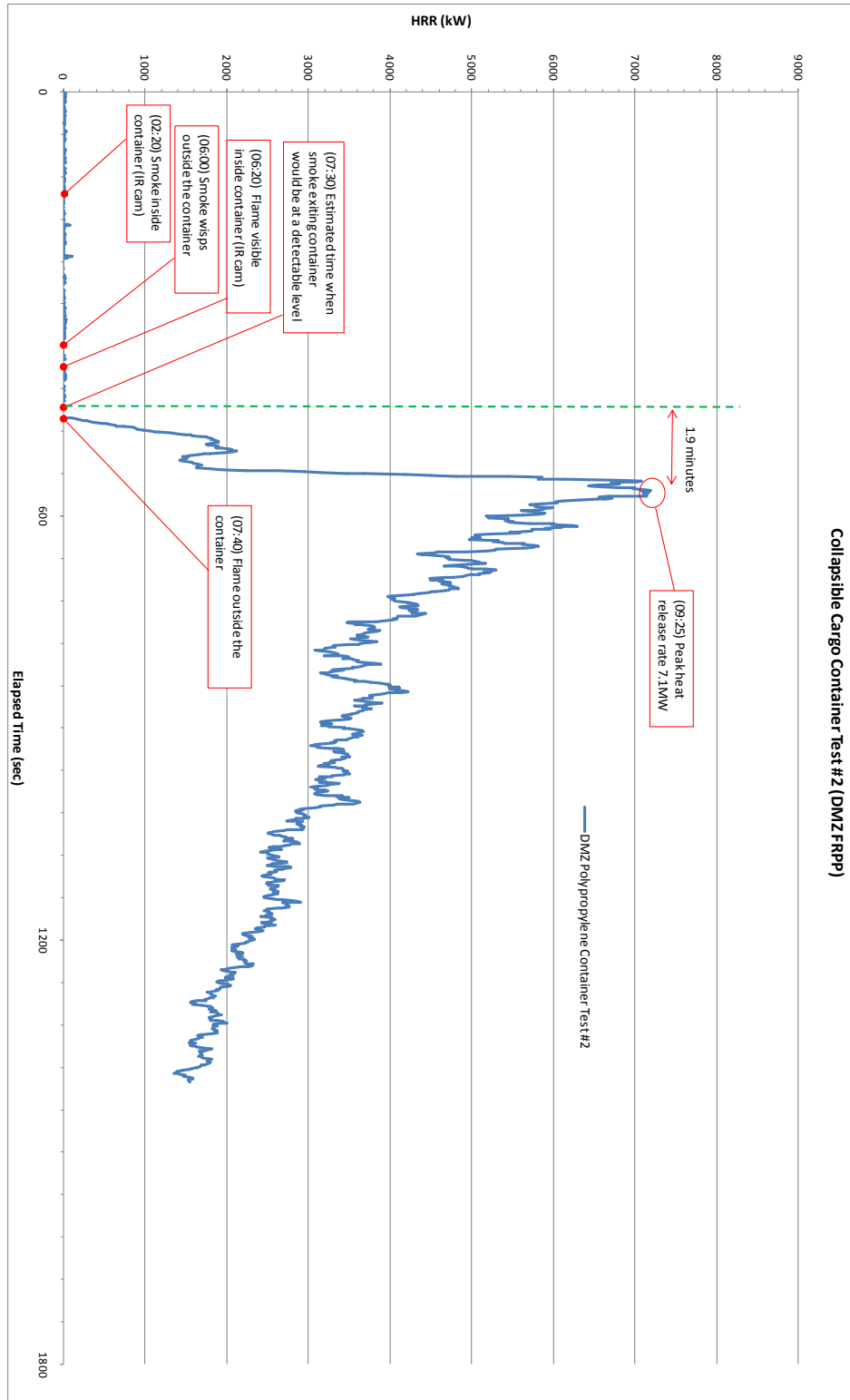


Figure 22: Energy release rate and observations from DMZ container test 2

D. SUMMARY AND CONCLUSIONS

The small scale tests involving single battery cells established values for the total energy release and the peak energy release rate for a few types of batteries when tested using the ASTM E1354 calorimeter. The total energy released per battery cell when normalized by the battery's weight is generally less than most ordinary combustibles. The peak energy release rate of the batteries did not appear to be influenced by the calorimeter's imposed heat flux to the battery samples. The batteries behaved more like balloons containing a flammable substance and, upon rupture of the balloon, quickly expelling the flammable contents as opposed to traditional materials whose burning rate is strongly dependent on the external heat flux they receive. The imposed heat flux did have a strong influence on the time to failure (or venting) on all the types of batteries tested.

In the intermediate scale tests conducted using single boxes containing 100 batteries each, exposed to a 30kW propane burner, the batteries increased the fire's energy release rate by approximately 90kW at the peak burning rate. This increase, based on the data from the small scale tests, was equivalent to seven battery cells failing simultaneously. During the test, while the batteries were venting, some of the burning batteries became projectiles, landing a few feet away from their original position.

In the intermediate scale tests conducted using single boxes containing 100 batteries each and an additional fire load of 18 cardboard boxes containing shredded paper, the batteries were found to be capable of spreading the fire to adjacent combustible materials. Upon causing ignition, the presence of batteries in the fire load did not appear to have an influence on the characteristics of the fire. Ignition of vented battery electrolyte caused an explosion, which resulted in the opening of the closure flaps of a cardboard box in which the box of batteries was placed. This explosion, which opened the box, allowed oxygen to enter, facilitating the combustion process.

Overall, from the small scale and intermediate scale tests, batteries of the 18650 lithium-ion type, either singularly or in small quantities, have the potential to initiate a fire while not adding significantly to the fire load and intensity of the fire. Lithium and lithium-ion polymer batteries behaved similarly in small scale single cell tests but were not tested at the intermediate scale level.

From the tests involving batteries, the following conclusions were made:

- At the single-cell level, the energy release rate of lithium and lithium-ion type batteries is relatively small when compared to other ordinary materials.
- In addition to the energy release from batteries resulting in combustion, there is an associated mechanical energy release. This mechanical energy release is capable of compromising the integrity of packaging and creating incendiary projectiles.

- Lithium (primary) batteries tend to exhibit more energetic failures than lithium-ion (secondary) batteries.
- The total energy release of a box of 100 lithium-ion batteries can be fairly accurately predicted based on single battery cell calorimetry data.
- The thermal runaway of lithium-ion batteries is capable of spreading from cell to cell within a package of batteries.
- The thermal runaway of lithium-ion batteries is capable of causing adjacent combustibles to ignite.

The large scale tests involving cargo containers established the total energy release and peak energy release rate for a standard fire load using two different types of containers. Although the standard fire load chosen may not be entirely representative of what can be found in a container of commercial cargo, it is a start for assessing the threat to an aircraft from a cargo container fire. It was observed that, based on container design and method of usage while in operation, there can be a vast difference in fire performance from one container type to another. This difference was observed in both the time that it took for a fire inside a container to become detectable and in the overall size and growth rate of the fire.

In the two tests with the A2N containers, sufficient smoke to activate an alarm began to exit the containers at 3 minutes 19 seconds and 2 minutes 30 seconds, respectively for the two tests, after smoke was visible within the containers. In the two tests with the collapsible DMZ containers, sufficient smoke to activate an alarm began to exit the containers at 18 minutes 30 seconds and 5 minutes 10 seconds, respectively for the two tests, after smoke was visible within the containers. The FAA regulation for cargo compartments certified with smoke detection (14 CFR 25.858) requires a 1 minute detection time from the start of a fire. The regulation does not account for any delay in detection caused by the container. Current certification tests do not use containers.

The time interval between the time when sufficient smoke to trigger an alarm was exiting the containers to the time when the container fires were at their peak energy release rates was significantly different for the two types of containers tested. For the A2N containers, this time interval was 7.5 and 10.5 minutes, while for the collapsible DMZ containers, this time interval was 2.2 and 1.9 minutes. Particularly in the case of the collapsible DMZ containers, this short time interval between a fire being detectable and peak energy release rate precludes any mitigating action to suppress the fire and protect the aircraft structure. Although 14 CFR 25.858 for cargo compartments certified with smoke detection does not specify any performance metric for what goes on after detection, the results of these fire tests suggest that the intent of the regulation as stipulated in paragraph (b) of 14 CFR 25.858, "the system must be capable of detecting a fire at a temperature significantly below that at which the structural integrity of the airplane is substantially decreased," is not being met.

For the same fire load, the DMZ containers constructed out of fire-resistant polypropylene exhibited twice the peak energy release rate and total energy output than the A2N containers constructed out of aluminum and polycarbonate.

From the tests involving cargo containers, the following conclusions were made:

- Differences in container design and materials have a significant effect on fires originating within them.
- Container design has a significant effect on the time it takes for a fire to become detectable to an outside smoke detector.
- Container construction materials have a significant effect on the total fire load and energy release rate of a cargo fire.
- The time it takes to detect a fire originating within a cargo container exceeds the time specified in 14 CFR.
- The growth rate of container fires after they become detectable can be extremely fast, precluding any mitigating action.

Joseph Panagiotou
Fire & Explosion Investigator

E. APPENDIX A (COVER SHEET OF ACCOMPANYING DOCUMENT SHOWN)

Data From Lithium, Lithium-ion and Lithium-ion Polymer Battery Fire Tests Conducted at the FAATC

These tests were conducted using the ASTM E1354 standard for oxygen consumption calorimetry. Single battery cells were used for these tests.

Date	Mfg	Battery Type	Voltage VDC	Radiant Heat Flux kW/m2	Initial Vent (sec)	Final Vent (sec)	Peak HRR kW	Total HR kJ	Mass loss (g)	Total HR/mass loss kJ/g	Total Mass (g)	Total HR/Mass kJ/g	Comments	Data file
3/30/11	LG	18650	4.03	10	731	N/A	0.2	9	4	2.3	43.6	0.2		11030037
3/29/11	LG	18650	4.03	10										
3/29/11	LG	18650	4.03	30	165	242	13.7	84	10.3	8.2	43.6	1.9		11030039
3/29/11	LG	18650	4.03	30	186	242	9.8	76	12.6	6.0	43.6	1.7		11030040
3/9/11	LG	18650	4.03	50	109	159	10.2	100.2	10.1	9.9	43.6	2.3		11030010
3/9/11	LG	18650	4.03	50	96	137	16.2	92.8	9.6	9.7	43.6	2.1		11030011
3/9/11	LG	18650	4.03	75	56	75	12.3	81.6	9.1	9.0			No shield	11030003
3/9/11	LG	18650	4.03	75	63	82							No fare	11030004
3/9/11	LG	18650	4.03	75	50	71	16.2	92.6	9.1	10.2	43.6	2.1		11030005
	Titanium Innovations	CR2		10										
	Titanium Innovations	CR2		10										
3/29/11	Titanium Innovations	CR2	3.28	30	115	148	2.8	27	3.3	8.2	10.6	2.5		11030033
3/29/11	Titanium Innovations	CR2	3.24	30	118	161	3.1	32	3.2	10.0	10.6	3.0		11030034
3/9/11	Titanium Innovations	CR2	3.25	50	77	85	3.9	20.3	3.4	6.0	10.6	1.9		11030012
3/9/11	Titanium Innovations	CR2	3.2	50	90	118	3.7	33.1	3.5	9.5	10.5	3.2		11030013
3/9/11	Titanium Innovations	CR2	3.29	75	54	65	6.5	33.5	2.3	14.6	10.6	3.2		11030006
3/9/11	Titanium Innovations	CR2	3.26	75	54	70	4.2	31.4	3.7	8.5	10.8	2.9		11030007
	Sure Fire	SF123A		10										
	Sure Fire	SF123A		10										
3/29/11	Sure Fire	SF123A	3.23	30	104	149	4.2	42	4.7	8.9	16.3	2.6		11030031
3/29/11	Sure Fire	SF123A	3.23	30	113	149	3.6	55	8.4	6.5	16.4	3.4		11030032
3/9/11	Sure Fire	SF123A	3.23	50	74	94	3.9	52.2	4.4	11.9	16.5	3.2		11030014
3/9/11	Sure Fire	SF123A	3.23	50	69	89	4.7	73.5	4.4	16.7	16.4	4.5		11030015
3/9/11	Sure Fire	SF123A	3.23	75	48	68	5.9	64	3.8	16.8	16.4	3.9		11030008
3/9/11	Sure Fire	SF123A	3.24	75	52	67	3.5	46.6	4.3	10.4	16.4	2.7		11030009
3/30/11	Powerizer	PL-553562-10C	3.83	10	500	N/A	0.2	6	5.2	1.2	23.4	0.3		11030035
	Powerizer	PL-553562-10C	3.83	10										
3/29/11	Powerizer	PL-553562-10C	3.83	30	112	N/A	9.2	57	3.3	17.3	23.3	2.4		11030025
3/29/11	Powerizer	PL-553562-10C	3.83	30	130	N/A	8.9	47	2.9	16.2	23.2	2.0		11030026
3/29/11	Powerizer	PL-553562-10C	3.83	50	38	51	6	77	5.1	15.1	23.2	3.3		11030023
3/29/11	Powerizer	PL-553562-10C	3.83	50	48	63	5.7	75	5.6	13.4	23.3	3.2		11030024
3/28/11	Powerizer	PL-553562-10C	3.83	75	14	44	7.1	109	6.1	17.9	23.2	4.7		11030017
3/28/11	Powerizer	PL-553562-10C	3.83	75	22	31	5.8	97	7.2	13.5	23.3	4.2		11030018
3/30/11	Powerizer	PL-603495-10C	3.82	10	512	N/A	0.5	0	4.3	0.0	41.3	0.0		11030036
	Powerizer	PL-603495-10C	3.82	10										
3/29/11	Powerizer	PL-603495-10C	3.82	30	64	84	7.8	156	10.2	15.3	41.4	3.8		11030027
3/29/11	Powerizer	PL-603495-10C	3.82	30	88	88	7	145	9.8	14.8	41.5	3.5		11030028
3/28/11	Powerizer	PL-603495-10C	3.82	50	35	52	8	162	11.1	14.6	41.1	3.9		11030021
3/28/11	Powerizer	PL-603495-10C	3.82	50	35	59	5.8	147	11.1	13.2	40.8	3.5		11030022
3/28/11	Powerizer	PL-603495-10C	3.82	75	19	35	8.9	165	12.1	13.6	41.3	4.0		11030019
3/28/11	Powerizer	PL-603495-10C	3.82	75	22	39	7.4	170	12	14.2	41.3	4.1		11030020

F. APPENDIX B (COVER SHEET OF ACCOMPANYING DOCUMENT SHOWN)



Title	Calorimetry- Box of Lithium Batteries		
Test Type	Custom		
Lab Number	NTSB-2	Author	Justin L. Rowe
Test date	8/9/11	No. Tests	2

Table of Contents

Table of Contents..... 1

Introduction 2

Test Set Up..... 2

Experiment Details..... 4

Instrumentation..... 4

Results for Test 1 (Exp. ID 6552)..... 9

Results for Test 2 (Exp. ID 6553)..... 20

NOTE: All dimensional measurements were taken in English units and were later converted to metric units. Any inconsistencies between the two units are due to rounding errors when the English units were converted to metric.

G. APPENDIX C (COVER SHEET OF ACCOMPANYING DOCUMENT SHOWN)



Title	Calorimetry-Eighteen Cardboard Boxes		
Test Type	Custom		
Lab Number	NTSB-3	Author	Justin L. Rowe
Test dates	8/8/11, 8/9/11, 8/10/11	No. Tests	4

Table of Contents

Table of Contents 1

Introduction 2

Test Set Up 2

Experiment Details 6

Instrumentation 8

Results for Test 1 (Exp. ID 6548) 12

Results for Test 2 (Exp. ID 6549) 24

Results for Test 3 (Exp. ID 6557) 35

Results for Test 4 (Exp. ID 6558) 47

NOTE: All dimensional measurements were taken in English units and were later converted to metric units. Any inconsistencies between the two units are due to rounding errors when the English units were converted to metric.

H. APPENDIX D (COVER SHEET OF ACCOMPANYING DOCUMENT SHOWN)



Title	Calorimetry- Single Cardboard Box		
Test Type	Custom		
Lab Number	NTSB-1	Author	Justin L. Rowe
Test dates	8/8/11, 8/9/11	No. Tests	4

Table of Contents

Table of Contents 1

Introduction 2

Test Set Up 2

Experiment Details 3

Instrumentation 4

Results for Test 1 (Exp. ID 6539) 9

Results for Test 2 (Exp. ID 6543) 19

Results for Test 3 (Exp. ID 6544) 28

Results for Test 4 (Exp. ID 6555) 37

NOTE: All dimensional measurements were taken in English units and were later converted to metric units. Any inconsistencies between the two units are due to rounding errors when the English units were converted to metric.

I. APPENDIX E (COVER SHEET OF ACCOMPANYING DOCUMENT SHOWN)



Title	Calorimetry-Cargo Container Fires		
Test Type	Custom		
Lab Number	NTSB-4	Author	Justin L. Rowe
Test dates	8/10/11, 8/11/11	No. Tests	4

Table of Contents

Table of Contents 1

Introduction 2

Test Set Up 3

Experiment Details 5

Instrumentation 8

Results for Test 1 (Exp. ID 6561) 12

Results for Test 2 (Exp. ID 6562) 26

Results for Test 3 (Exp. ID 6564) 39

Results for Test 4 (Exp. ID 6565) 52

NOTE: All dimensional measurements were taken in English units and were later converted to metric units. Any inconsistencies between the two units are due to rounding errors when the English units were converted to metric.

J. REFERENCES

(2011, May 18). *Batteries & Battery-Powered Devices*. Retrieved 1 20, 2012, from www.faa.gov:

http://www.faa.gov/about/office_org/headquarters_offices/ash/ash_programs/hazmat/aircarrier_info/media/Battery_incident_chart.pdf

Webster, H. (June 2004). *Flammability Assessment of Bulk-Packed, Nonrechargeable Lithium Primary Batteries in Transport Category Aircraft*. Atlantic City, NJ: Federal Aviation Administration.

Webster, H. (October 27, 2010). Lithium-Ion and Lithium Metal Battery Update. *2010 Triennial Fire and Cabin Safety Conference*. Atlantic City, NJ: FAA.